Porous materials *via* egg-constituents templating

Valentin Valtchev,*[a] Feifei Gao[a] and Lubomira Tosheva[b]

Received (in Montpellier, France) 14th March 2008, Accepted 23rd June 2008
First published as an Advance Article on the web 4th July 2008
DOI: 10.1039/b804449j

The possibility to prepare porous materials with controlled composition and porous structure using environmentally benign, readily available and cheap templates such as egg-derived scaffolds was explored. Different parts of the egg were used for the preparation of: (i) porous disks and beads of SiO_2 and SiO_2–Al_2O_3; (ii) micro-/macroporous interwoven hollow tubes; (iii) hybrid eggshell membrane/zeolite structures; and (iv) zeolite/calcite composite. The synthesis conditions and the properties of obtained materials are discussed. The materials were characterized by XRD, SEM, N_2 adsorption measurements and chemical analysis.

Introduction

Porous silica and alumina solids have wide applications as catalyst supports, packing materials and membranes. Lately, a lot of research efforts have been dedicated to the development of novel methods for synthesis of porous solids and in particular towards the use of sacrificial templates which upon removal by calcination or chemical dissolution yield materials with controlled porosity. The preparation of solids with predetermined porous structure and chemical composition is challenging as such materials can conform to specific process requirements.

The multilevel organization of a synthetic hierarchical material is usually obtained by a sequential assembly of basic components. Considering that such syntheses can be dear, often involving the use of complicated synthesis procedures and/or equipment, the ability of nature to build complex biological specimens is simply amazing. This ability is based on the remarkable capability of biological organisms to recognize, sort and process different species by highly functional assemblies of proteins, nucleic acids and other macromolecules which carry out complicated tasks that are still challenging us to emulate. Thus, the biological concept gives inspiration for creating a new generation of synthetic materials and devices with advanced structures and functions. It should also be mentioned that there is growing interest in building hybrid materials by binding of biological molecules to technologically relevant surfaces. Thus, the number of interdisciplinary research projects at the frontier between materials science and biology has increased tremendously during the last decade. Consequently many review articles and textbooks devoted to this rapidly growing discipline have appeared recently.[1–10]

Besides the astonishing ability of self-organization and complex functionality, biological specimens are attractive with their shapes and patterns that are unapproachable by synthetic materials. These complex architectures combined with multilevel organization and narrow functionality of different parts inspires modern materials science. The organic chemistry, especially supramolecular chemistry, has been very successful in creating large superstructures of stunning morphology. In contrast, inorganic chemistry is still lagged behind. The intricate organic–inorganic reactions in biological specimens leading to multilevel inorganic constructions are far from being understood and simulated. Thus, the replication of biological samples is amongst the most widely used approaches for synthesis of inorganic materials with multilevel organization and complex morphology.[11–32]

The present study deals with the preparation of porous structures templated by egg-derived components. This raw material, which is cheap and readily available at any supermarket, was chosen to exemplify the enormous possibilities of building complex materials offered by nature. Egg-derived templates have already been used to prepare different synthetic solids.[33–41] The present study demonstrates that all parts of a hen egg can be employed in the preparation of porous solids with particular porous organization and morphological features.

Experimental

Materials

Eggs from hens were purchased from a local supermarket. Egg yolk and white were manually separated prior to use.

Colloidal silica sols Bindzil X/Y, where X is the concentration of SiO_2 and Y is the surface area with X/Y of 40/130, 30/220 15/550 (Eka Chemicals, Sweden) and alumina sol (10 wt% Al_2O_3) prepared from Disperal P2 (Sasol, surface area of 260 m^2 g^{-1}) were used as silica and alumina precursors, respectively.

Polycation agent (poly(diallyldimethylammonium chloride), 20 wt% aqueous solution, Aldrich) diluted to 1 wt% with distilled water was used to reverse the negative surface charge of eggshells and egg-shell membranes prior to zeolite seed adsorption.

Silicalite-1 nanocrystal suspensions were prepared by employing tetraethylorthosilicate (TEOS, Merck), tetrapropylammonium (TPA) hydroxide (20% in water, Merck) and distilled water. After mixing of the reactants, the solution

[a] *Laboratoire de Matériaux à Porosité Contrôlée, UMR-7016 CNRS, ENSCMu, Université de Haute Alsace, 3, rue Alfred Werner, 68093 Mulhouse, France. E-mail: Valentin.Valtchev@univ-mulhouse.fr*
[b] *Division of Chemistry and Materials, Manchester Metropolitan University, Chester Street, Manchester, UK M1 5GD*

was allowed to hydrolyze for 14 h and was then treated hydrothermally at 90 °C for 24 h. The starting composition of the clear solution used for the synthesis was: 4.5 $(TPA)_2O$: 25 SiO_2 : 480 H_2O : 100 EtOH. The presence of ethanol (EtOH) in this composition is a consequence of the use of TEOS as a silica source. After the synthesis, the zeolite suspension was purified by four series of high-speed centrifugations (20 000 rpm, 1 h), decanting and redispersion in distilled water by ultrasonic treatment. The zeolite content in the seeding suspensions was adjusted to 1.0 wt% and the pH to 9.5 by adding 0.1 M ammonia solution.

Preparation of porous SiO_2 and SiO_2–Al_2O_3 spheres and discs

Egg yolk, colloidal silica and alumina particles were mixed in different proportions. A certain amount of water was also added to the mixture to obtain a gel with the desired viscosity. The mixtures were magnetically stirred for 30 min and then transferred into a crucible. To remove the template, the samples were first dried at 200 °C and then calcined at 600 °C for 5 h. Alternatively, the mixtures were loaded in syringes and dropwise frozen in liquid nitrogen, directly placed in a preheated to 600 °C furnace and heated for 5 h.

Micro-/macroporous materials issued from eggshell membranes

ZSM-5 films were grown on eggshell membranes by secondary growth of preliminary adsorbed seeds. First, the support was treated with a cationic polymer agent. Then negatively charged seeds were electrostatically adsorbed on the support. Both, inner membrane manually separated after boiling of the egg and eggshells comprising outer membrane were treated. The secondary growth was performed at 150 °C for 20 h with a solution having the following molar composition 1.5 $(TPA)_2O$: 0.25 Al_2O_3 : 25 SiO_2 : 1500 H_2O : 100 EtOH. After the secondary growth, the eggshell membrane from the eggshell membrane/zeolite composite was eliminated by calcination at 600 °C for 8 h. When eggshells were used, they were dissolved in 2 M HCl in order to obtain the eggshell membrane/zeolite composite.

Silicalite-1 film synthesis on eggshell supports

The eggshells were pre-treated in a similar way as described above and subjected to secondary growth under identical conditions. After cooling, the composites were treated with 0.1 M ammonia solution in an ultrasonic bath for 10 min to remove the loosely attached silicalite-1 crystals, rinsed repeatedly with distilled water and dried at 80 °C. The composite was calcined at 550 °C for 6 h in air.

Organic template-free ZSM-5/eggshell membrane hybrid synthesis

In order to obtain an inorganic/organic hybrid that did not require calcination, organic template-free synthesis of ZSM-5 was performed. The composition of the initial gel was: 11.5 Na_2O : 3 Al_2O_3 : 100 SiO_2 : 2700 H_2O. The synthesis were performed at 165 °C for 20 h. The product was recovered by suction filtration and drying at 60 °C overnight.

Characterization

The obtained materials were studied by X-ray diffraction (XRD) using a STOE STADI-P diffractometer in Debye-Scherrer geometry equipped with a linear position-sensitive detector (6° in 2θ) and employing Ge-monochromated Cu-Kα_1 radiation. Electron micrographs were taken on a Philips XL30 FEG scanning electron microscope (SEM). The TEM images were taken with a Philips CM200 operating at 200 kV and using a LaB_6 crystal as an electron source. Nitrogen adsorption measurements were carried out on a Micromeritics ASAP 2010 surface area analyzer. The calcined samples were analyzed after outgassing at 300 °C. The elemental analyses of the core crystals were performed on an X-ray fluorescence spectrometer MagiX (Philips). Prior to the analysis the powdery sample was melted with $Li_2B_4O_7$ at 1300 °C. The resultant glass bead was analyzed under vacuum with a Rhodium anticathode (2.4 kW). Particles size analysis was performed by dynamic light scattering (DLS) with a Malvern ZetaSizer Nano ZS instrument. Zeta potential measurements were performed with the same instrument using a folded capillary cell (DTS1060).

Results and discussion

Porous structures built by yolk templating

This part of the study reports on the preparation of pure silica and mixed silica–alumina porous structures obtained by egg yolk templating. Egg yolk consists 68% low-density lipoproteins (LDL), 16% high-density lipoproteins (HDL), 10% livetins and 4% phosvitins.[42] LDL are large spherical particles of about 35 nm diameter. Yolk constituent ability to form emulsions in water or to interact, following heat treatment, and form network structures exhibiting viscoelasticity is well known.[43,44] Templating behaviour of biomolecules depends on the intimate mixing with inorganic precursor particles. Thus, functional behaviour of dominant yolk constituents, that is, the proteins and their physical interactions with nanosized inorganic precursors is of paramount importance for the preparation of precursor composite material and its successful transformation into a porous structure with controlled characteristics. The surface charge of yolk constituents and precursor silica and alumina particles were studied in aqueous media at different pH values. The obtained results are summarized in Table 1. As can be seen at low and intermediate pH values some difference in the surface charge of biomolecules and inorganic particles were found. For instance in acidic media (pH = 2.2) the alumina particles; egg yolk and white showed positive ζ potential, whereas a negative value close to

Table 1 Zeta potential (mV) of inorganic precursors and egg constituents at different pH values

	pH		
Material	2.2	5.3	9.1
Bindzil 30/220	−3	−13	−42
Disperal P2	+64	+51	−27
Egg yolk	+12	−8	−47
Egg white	+26	−11	−33

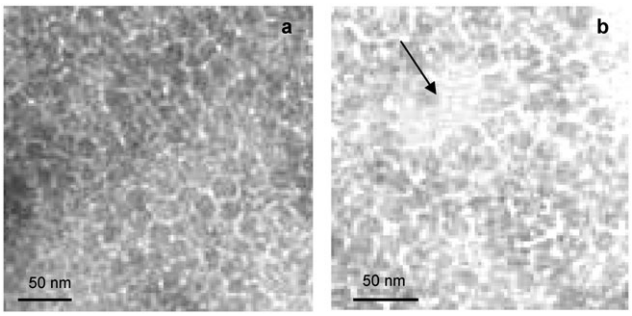

Fig. 1 High-resolution TEM images of silica mesoporous material prepared by egg yolk templating.

zero was recorded for the silica ones, which is due to the fact that the isoelectric point of silica is in the pH range 2–4. Except for alumina, all other species showed a negative surface charge at pH = 5.3. In basic media both inorganic particles and egg yolk and white constituents were negatively charged as the surface charge for silica and alumina particles was −42 and −27, respectively. The values for egg yolk and white varied in the same range, that is, −47 for egg yolk and −33 for egg white. Based on these data initial mixtures with similarly charged particles were prepared. In other words basic media was used for all preparations. The fact that both inorganic precursor particles and templating biomolecules were negatively charged prevented uncontrolled aggregation. Consequently, mixtures with uniformly distributed inorganic and organic parts were obtained. The mixtures were vigorously stirred for 1 h and then the temperature was slowly increased to 70 °C upon continuous stirring. The latter causes partial cross linking of egg proteins and formation of a network embedding the inorganic precursors. Thus, during the high-temperature sintering step the coalescence between particles is minimized and oxygen bridges are formed in a limited part of the particles surface. TEM micrographs showing uniform distribution of silica nanoparticles after such a preparation are presented in Fig. 1. Besides small mesopores between uniformly distributed silica particles (Fig. 1(a)) larger cavities as a consequence of proteins organized into granular structures (Fig. 1(b)) were observed.

Macromorphological features of porous yolk-templated structures can be easily controlled by chosen the form of the vessel used for high-temperature sintering. For instance, disk-like structures with a size predetermined by the crucible used were obtained after drying and calcination of the hybrid materials. Spherical macrostructures of various sizes were prepared by freezing drops of the yolk–silica or yolk–alumina–silica precursor in liquid nitrogen followed by calcination at elevated temperature (Fig. 2). Nitrogen adsorption measurements revealed certain differences between silica and silica–alumina spheres. It seems that the silica particles undergo coalescence during the preparation, independently of the heating procedure employed, *i.e.* preliminary drying at 200 °C followed by treatment at 600 °C or direct calcination at 600 °C. Specific surface areas of *ca.* 90 $m^2 g^{-1}$ were obtained in both cases, which were lower than the specific surface area of the initial silica particles. The adsorption isotherm is close to type II, which is typical of nonporous or macroporous materials (Fig. 3(a)). The hysteresis at high relative pressure is indicative of the generated intercrystalline mesoporosity. Indeed, BJH pore size analysis revealed the presence of large meso- and macropores in the range 200–1000 Å (Fig. 3(b)). It should also be mentioned that similar BET surface areas were obtained for samples prepared using different egg yolk to silica weight ratios.

Silica–alumina structures prepared by mixing yolk, silica (Bindzil 30/220) and alumina source (Dispersal P2) at 1 : 1 : 0.5 weight ratio showed larger specific surface areas, in the range 200–250 $m^2 g^{-1}$, than the corresponding silica structures. The recorded isotherm was a combination of type II and IV with a clearly distinguishable mesoporous part (Fig. 3(c)). Correspondingly a much narrower pore size distribution (Fig. 3(d)) compared to the all-silica sample (Fig. 3(b)) was observed. The main pore fraction was in the range 50–500 Å with a maximum around 150 Å. The differences between the silica and the silica–alumina structures obtained *via* yolk templating indicate that the presence of alumina prevents the sintering of the silica particles and that materials of large surface areas can be obtained. It is worth recalling that the yolk plays the role of a sacrificial template that provides the mesoporous characteristic of the material. Most of the experiments in this study were performed with egg yolk. We have also tested the possibility to build porous structures using egg white (albumen), a material also rich of proteins that offers the advantage of easy emulsifying and foaming. Porous structures similar in pore size distribution and total surface area to those obtained with yolk were obtained. Albumen templated structures, however, were brittle compared to their yolk-templated counterparts.

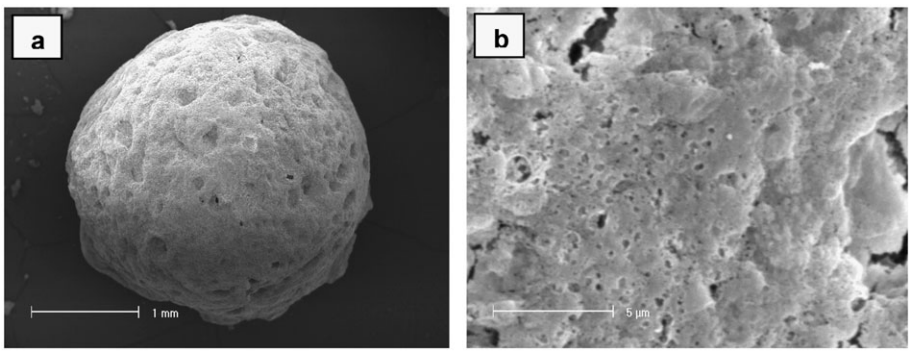

Fig. 2 General (a) and close-up (b) SEM views of a spherical structure prepared by yolk templating of a silica–alumina colloidal precursor.

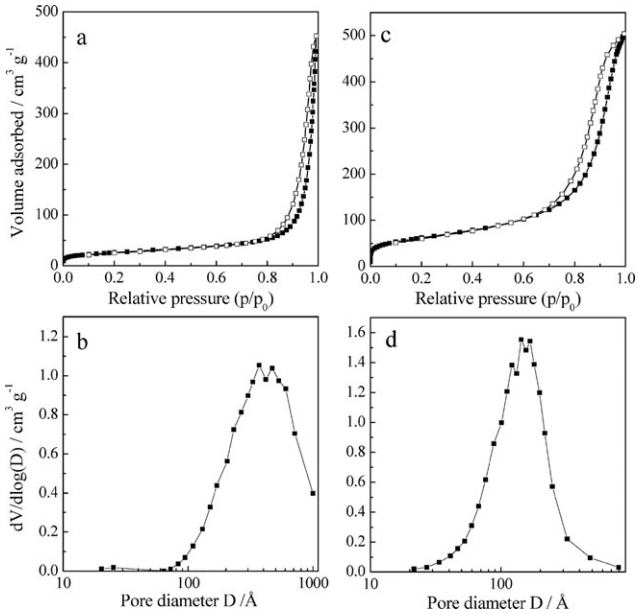

Fig. 3 N_2 adsorption/desorption isotherm (a) and BJH desorption pore size distribution (b) for a calcined sample prepared with Bindzil 30/220 precursor and calcined at 600 °C after a liquid-nitrogen shaping procedure. N_2 adsorption/desorption isotherm (c) and BJH desorption pore size distribution (d) for a silica–alumina sample prepared with Bindzil 30/220 and Dispersal P2 precursors and calcined at 600 °C after a liquid nitrogen shaping procedure.

Micro-/macroporous structures by eggshell membrane templating

A major drawback in the use of microporous zeolite-like materials in processing bulky molecules is the channel blocking. Thus, solutions that might circumvent this disadvantage are highly desired. The use of zeolite nanocrystals[45] or conventional micrometer sized crystals comprising mesopores[46] is amongst the most largely exploited approaches. Materials with bimodal micro-/macropore systems involving zeolites are also of considerable interest, since they combine the benefits of each pore size regime. This part of the study is devoted to the preparation of such a material by eggshell membrane templating. The replication of the interwoven shell membrane filaments offers the advantage of an interconnected network of macropores.

The shell membranes, formed in the isthmus region of the avian oviduct, are two dense nets of fibrils composed of a core surrounded by a fuzzy material referred to as a mantle.[47] The inner shell membrane, contacting the albumen, has thinner fibrils than the outer one. Both membranes are stable in basic media and were employed in the preparation of micro-/macroporous networks. The inner membrane was separated from albumen after boiling the egg, whereas outer one was subjected to zeolitization as attached to the eggshell.

In order to circumvent the incompatibility between the biological template and zeolite precursor mixture, nanosized zeolites seeds were employed to promote the crystallization on the eggshell membrane. According to the DLS analysis seeds with an average size of about 60 nm and a narrow particle size distribution were employed. Zeta potential measurements

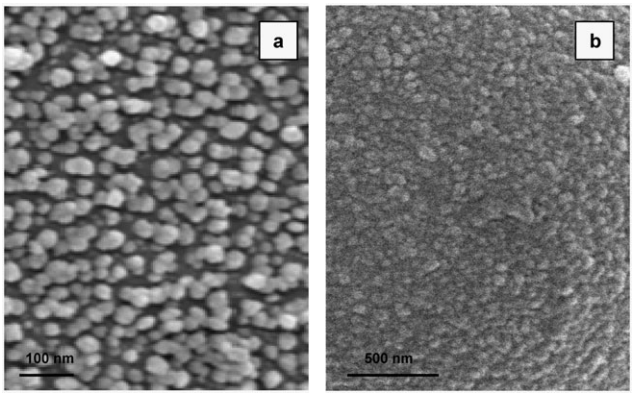

Fig. 4 Nanosized silicalite-1 seeds electrostatically adsorbed on an eggshell membrane: (a) one-step adsorption; and (b) two-step adsorption.

showed that both seeds and the inner membrane particles possess a negative charge in basic media (pH = 9.5). A polycation agent was employed to reverse the surface charge of eggshell membrane and a monolayer of nanoseeds was adsorbed on the surface (Fig. 4(a)). Repeating the procedure leads to formation of an extended layer of zeolite seeds which entirely covers the support (Fig. 4(b)). The same pre-treatment procedure was employed for the preparation of ZSM-5 film on egg shells (*vide supra*). Pre-seeded support was subjected to hydrothermal treatment in a precursor mixture yielding a MFI-type zeolite. The adsorbed nanoseeds successfully promoted zeolite crystallization on the eggshell membrane and thus an extended intergrown layer covering the membrane network was obtained. Fig. 5(a) represents a part of eggshell with the outer membrane. Fig. 5(b) shows a high-magnification micrograph of the fibrils building the inner membrane. A general view of a part of the outer membrane covered with a zeolite layer is shown in Fig. 5(c). After calcination at 600 °C for 8 h the membrane undergoes pyrolysis and a macroporous structure representing a zeolite negative replica of the interwoven membrane is obtained (Fig. 5(d)). The piece of the inner membrane after calcination was subjected to XRD analysis (Fig. 6), which revealed that the walls of the macroporous tubes were built by a highly crystalline MFI-type material (ZSM-5). The specific surface area of the material was 408 m^2 g^{-1} that further confirmed the high crystallinity of material. The Si/Al ratio of the obtained material was 34.

Flexible eggshell membrane/zeolite composites

The procedure employed for the preparation of micro-/macroporous materials was applied for the preparation of eggshell membrane/zeolite composites. A gel composition yielding ZSM-5 without using an organic structure directing agent (SDA) was employed.[48] Thus, the calcination step to open up the zeolite micropore structure was omitted. ZSM-5 material deposited according to this procedure was much more abundant and thus the spaces between the cone-like structures supporting outer membrane (Fig. 5(a)) were filled up with zeolite. After the hydrothermal treatment the obtained composite was subjected to acid treatment into 2 M HCl overnight, which resulted in complete dissolution of the eggshell. The

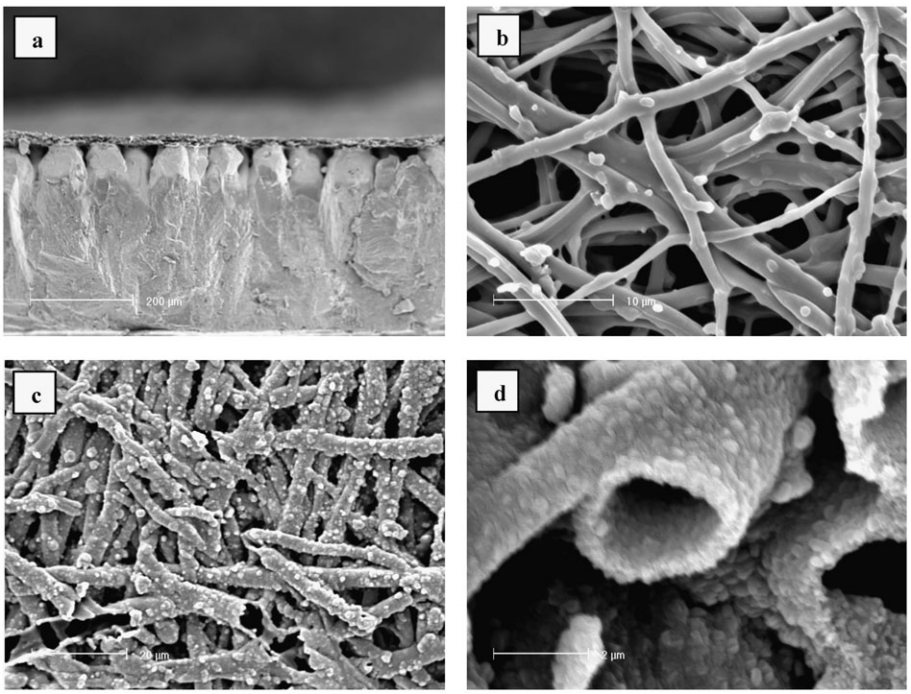

Fig. 5 SEM micrographs of: (a) part of eggshell with outer membrane; (b) close-up SEM view of an inner membrane; (c) general view of outer membrane covered with a layer of intergrown MFI-type materials; and (d) close-up view of calcined inner membrane where macropores formed by replication of the eggshell membrane can be seen.

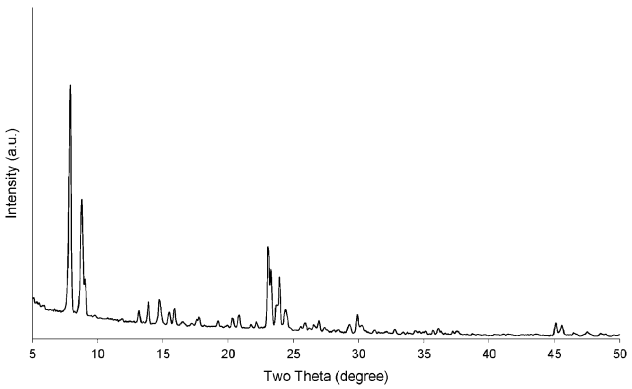

Fig. 6 XRD pattern of ZSM-5 micro-/macroporous material prepared by replication of the inner eggshell membrane.

SEM inspection showed that the eggshell membrane survived the severe acid treatment and supported the intergrown zeolite structures obtained during the crystallization stage (Fig. 7(a) and (b)). The zeolite seems to be firmly attached to the membrane surface since bending of the membrane did not result in zeolite detachment. A closer look on the deposited zeolite structures revealed that the base was broad and became thinner to the top (Fig. 7(c)), where the individual crystals (300–600 nm) building the intergrown zeolite bodies can be distinguished (Fig. 7(d)).

Zeolite-functionalized eggshell support

Eggshells have a highly ordered and mineralized structure, which contains between 95 and 97% $CaCO_3$. This high purity calcite is a raw material for a number of applications such as animal feed supplement, papermaking additive and pharmaceutical ingredients. More advanced uses could be envisaged after some modification of the surface of the eggshell. For instance, calcite supports are employed in catalysis and an increase of the specific surface area may result in a material with interesting properties. Eggshells in the present work were functionalized by deposition of a thin silicalite-1 layer on the surface by a seeding procedure followed by secondary growth. Thin well intergrown zeolite layer covers the eggshell (Fig. 8(a)). The uniformity and density of the silicalite-1 film can be clearly seen in Fig. 8(b).

Conclusions

The present study exemplified the large possibilities offered by biological templates in the preparation of porous materials. Using different parts of eggs from hen the following porous materials were obtained:

- Self supported disks and beads with distinct porous features built of silica or silica–alumina particles;
- Micro-/macroporous all-zeolite material that combine two distinct pore size regions;
- Hybrid composites, where eggshell membrane plays the role of a flexible support of intergrown zeolite structures built of nanoparticles;
- Calcite/zeolite composites of a thin zeolite film grown on calcite eggshell supports.

The series of porous materials obtained using templates that are easily available are a sound proof for the enormous possibilities offered by nature in the area of materials science. Besides the complex morphology and multilevel organization of the prepared materials, the natural templates used in this

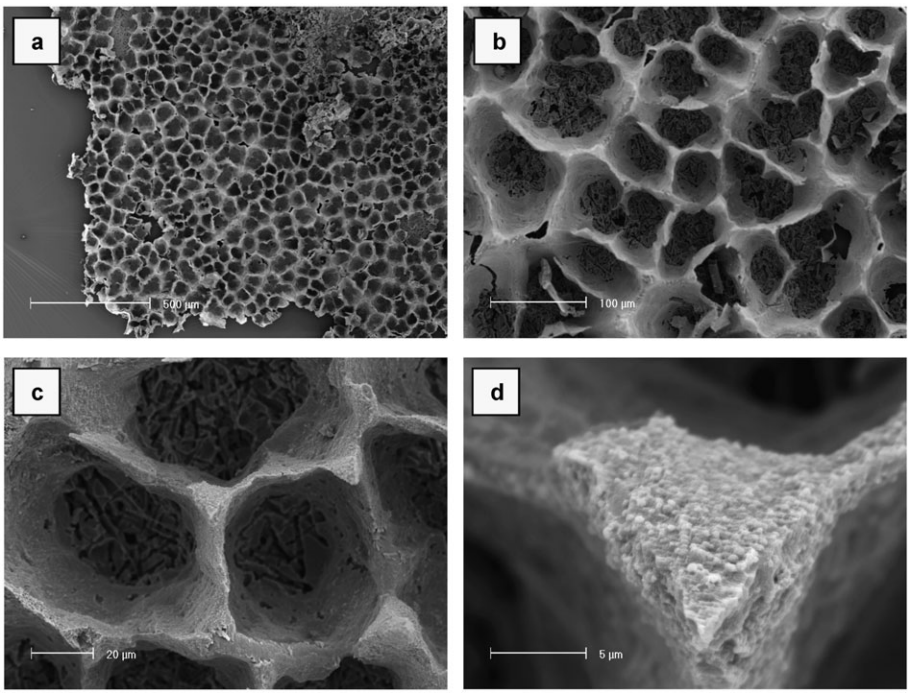

Fig. 7 Eggshell membrane/zeolite hybrid, where the zeolite part replicates the cone-like $CaCO_3$ structure at the internal surface of eggshells while the eggshell membrane supports the zeolite deposited during hydrothermal treatment.

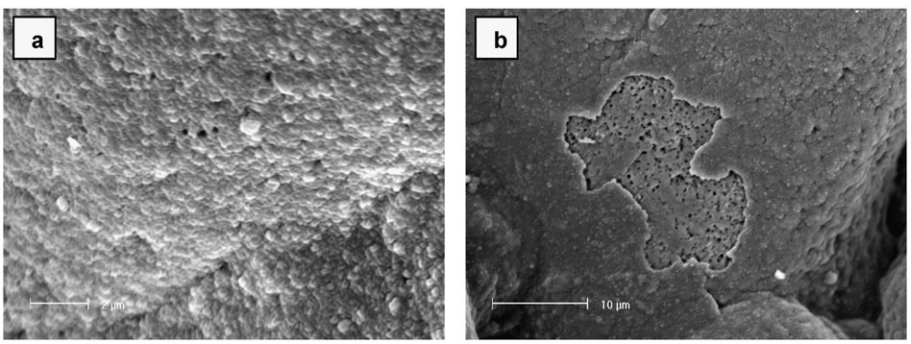

Fig. 8 (a) High-magnification SEM micrograph of silicalite-1 film obtained by secondary growth. (b) Destroyed part of the silicalite-1 film, where the uniformity of the intergrown layer can be seen.

work are environmentally benign and inexpensive. Last but not least, all parts of this complex biological material were employed in the preparation of porous solids, which further evidences the versatility of the bio-templates.

References

1. M. Sarikaya and I. A. Aksay, *Biomimetics: Design and Processing of Materials*, AIP Press, New York, 1995.
2. S. Mann, *Biomineralization: Principle and Concepts in Bioinorganic Materials Chemistry*, Oxford University Press, Oxford, 2001.
3. E. Dujardin and S. Mann, *Adv. Mater.*, 2002, **14**, 775–788.
4. C. M. Niemeyer, *Angew. Chem., Int. Ed.*, 2001, **40**, 4128–4158.
5. A. Zampieri, W. Schwieger, C. Zollfrank and P. Greil, in *Handbook of Biomineralization: Biomimetic and Bioinspired Chemistry*, Wiley-VCH Verlag, Weinheim, Germany, 2007, pp. 255–288.
6. O. Takai, *Ann. N. Y. Acad. Sci.*, 2006, **1093**(Progress in Convergence), 84–97.
7. A. Weber, C. Gruber-Traub, M. Herold, K. Borchers and G. E. M. Tovar, *NanoS*, 2006, **2**, 20–27.
8. H. Sieber, *Mater. Sci. Eng., A*, 2005, **412**, 43–47.
9. P. Fratzl, *J. R. Soc. Interface*, 2007, **4**, 637–642.
10. R. Chen and J. A. Hunt, *J. Mater. Chem.*, 2007, **17**, 3974–3979.
11. J. N. Cha, G. D. Stucky, D. E. Morse and T. J. Deming, *Nature*, 2000, **403**, 289–292.
12. D. Volkmer, S. Tuguli, M. Fricke and T. Nielsen, *Angew. Chem., Int. Ed.*, 2003, **42**, 56–61.
13. E. G. Vrieling, T. P. M. Beelen, R. A. Van Santen and W. W. C. Gieskes, *J. Biotechnol.*, 1999, **70**, 41–53.
14. N. Kröger, R. Deutzmann and M. Sumper, *Science*, 1999, **286**, 1129–1132.
15. N. Kröger, R. Deutzmann and M. Sumper, *J. Biol. Chem.*, 2001, **276**, 26066–26070.
16. F. Noll, M. Sumper and N. Hampp, *Nano Lett.*, 2002, **2**, 91–95.
17. S. A. Crawford, M. J. Higgins, P. Mulvaney and R. Wetherbee, *J. Phycol.*, 2001, **37**, 543–554.
18. T. Coradin and J. Livage, *Colloids Surf., B*, 2001, **21**, 329–336.
19. V. Valtchev, M. Smaihi, A.-C. Faust and L. Vidal, *Angew. Chem., Int. Ed.*, 2003, **42**, 2783–2785.
20. V. Valtchev, M. Smaihi, A.-C. Faust and L. Vidal, *Stud. Surf. Sci. Catal., A*, 2004, **154**, 588–592.
21. V. Valtchev, M. Smaihi, A.-C. Faust and L. Vidal, *Chem. Mater.*, 2004, **16**, 1350–1355.

22. J.-M. Qian, J.-P. Wang and Z.-H. Jin, *Mater. Chem. Phys.*, 2003, **82**, 648–653.
23. K. Vyshnyakova, G. Yushin, L. Pereselentseva and Y. Gigotsi, *Int. J. Appl. Ceram. Technol.*, 2006, **3**, 485–490.
24. T. L. Y. Cheung and D. H. L. Ng, *J. Am. Ceram. Soc.*, 2007, **90**, 559–564.
25. J.-W. Kim, S.-W. Myong, H.-C. Kim, J.-H. Lee, Y.-G. Jung and Ch.-Y. Jo, *Mater. Sci. Eng., A*, 2006, **A434**, 171–177.
26. D. A. Streitwieser, N. Popovska and H. Gerhard, *J. Eur. Ceram. Soc.*, 2006, **26**, 2381–2387.
27. J.-M. Qian and Z.-H. Jin, *J. Eur. Ceram. Soc.*, 2006, **26**, 1311–1316.
28. D. A. Streitwieser, N. Popovska, H. Gerhard and G. Emig, *J. Eur. Ceram. Soc.*, 2005, **25**, 817–828.
29. C. Zollfrank and H. Sieber, *J. Eur. Ceram. Soc.*, 2004, **24**, 495–506.
30. H. Sieber, E. Vogli, F. Muller, P. Greil, N. Popovska and H. Gerhard, *Key Eng. Mater.*, 2002, 206–213.
31. E. Vogli, J. Mukerji, C. Hoffman, R. Kladny, H. Sieber and P. Greil, *J. Am. Ceram. Soc.*, 2001, **84**, 1236–1240.
32. P. Greil, T. Lifka and A. Kaindl, *J. Eur. Ceram. Soc.*, 1998, **18**, 1975–1983.
33. D. Yang, L. Qi and J. Ma, *Adv. Mater.*, 2002, **14**, 1543–1546.
34. Q. Dong, H. Su, D. Zhang, Z. Liu and Y. Lai, *Microporous Mesoporous Mater.*, 2007, **98**, 344–351.
35. Q. Dong, H. Su, W. Cao, D. Zhang, Q. Guo and Y. Lai, *J. Solid State Chem.*, 2007, **180**, 949–955.
36. Q. Dong, H. Su, D. Zhang, N. Zhu and X. Guo, *Scr. Mater.*, 2006, **55**, 799–802.
37. D. Yang, L. Qi and J. Ma, *J. Mater. Chem.*, 2003, **13**, 1119–1123.
38. Q. Dong, H. Su, J. Xu, D. Zhang and R. Wang, *Mater. Lett.*, 2007, **61**, 2714–2717.
39. P. K. Ajikumar, R. Lakshminarayanan and S. Valiyaveettil, *Cryst. Growth Des.*, 2004, **4**, 331–335.
40. J.-K. Liu, Q.-S. Wu, Y.-P. Ding and S.-Y. Wang, *J. Mater. Res.*, 2004, **19**, 2803–2806.
41. J. Liu, Q. Wu and Y. Ding, *J. Cryst. Growth*, 2005, **279**, 410–414.
42. M. Anton, V. Martinet, M. Dalgalarrondo, V. Beaumal, E. David-Briand and H. Rabersena, *Food Chem.*, 2003, **83**, 175–183.
43. V. Kiosseoglou, *Curr. Opin. Colloid Interface Sci.*, 2003, **8**, 365–370.
44. M. Anton and G. Gandener, *Colloids Surf., B*, 1999, **12**, 351–358.
45. L. Tosheva and V. Valtchev, *Chem. Mater.*, 2005, **17**, 2494–2513.
46. K. Egeblad, C. H. Christensen, M. Kustova and C. H. Christensen, *Chem. Mater.*, 2008, **20**, 946–960.
47. M. S. Fernandez, M. Araya and J. L. Arias, *Matrix Biol.*, 1997, **16**, 13–20.
48. S. D. Kim, S. H. Noh, J. W. Park and W. J. Kim, *Microporous Mesoporous Mater.*, 2006, **92**, 181–188.